Electrochemical sensing of glucose by chitosan modified graphene oxide

JPhys Materials

PAPER

Electrochemical sensing of glucose by chitosan modified graphene oxide

Fabrizio Poletti[1], **Laura Favaretto**[2], **Alessandro Kovtun**[2], **Emanuele Treossi**[2], **Franco Corticelli**[3], **Massimo Gazzano**[2], **Vincenzo Palermo**[2,4,5], **Chiara Zanardi**[1,2,5] and **Manuela Melucci**[2,5]

[1] Department of Chemical and Geological Sciences, University of Modena and Reggio Emilia, Modena, Italy
[2] Institute of Organic Synthesis and Photoreactivity, National Research Council of Italy, Bologna, Italy
[3] Institute for Microelectronics and Microsystems, National Research Council of Italy, Bologna, Italy
[4] Industrial and Materials Science, Chalmers University of Technology, Göteborg, Sweden
[5] Authors to whom any correspondence should be addressed.

E-mail: vincenzo.palermo@isof.cnr.it, chiara.zanardi@unimore.it and manuela.melucci@isof.cnr.it

Keywords: graphene oxide, nanocomposites, glucose sensing

OPEN ACCESS

RECEIVED
10 August 2019

REVISED
18 November 2019

ACCEPTED FOR PUBLICATION
2 December 2019

PUBLISHED
14 January 2020

Abstract

Graphene oxide (GO) coated electrodes provide an excellent platform for enzymatic glucose sensing, induced by the presence of glucose oxidase and an electrochemical transduction. Here, we show that the sensitivity of GO layers for glucose detection redoubles upon blending GO with chitosan (GO +Ch) and increases up to eight times if covalent binding of chitosan to GO (GO−Ch) is exploited. In addition, the conductivity of the composite material GO−Ch is suitable for electrochemical applications without the need of GO reduction, which is generally required for GO based coatings. Covalent modification of GO is achieved by a standard carboxylic activation/amidation approach by exploiting the abundant amino pendants of chitosan. Successful functionalization is proved by comparison with an ad-hoc synthesized control sample realized by using non-activated GO as precursor. The composite GO−Ch was deposited on standard screen-printed electrodes by a drop-casting approach. Comparison with a chitosan-GO blend and with pristine GO demonstrated the superior reliability and efficiency of the electrochemical response for glucose as a consequence of the high number of enzyme binding sites and of the partial reduction of GO during the carboxylic activation synthetic step.

1. Introduction

Chitosan (Ch, scheme 1) is a natural cationic polysaccharide, deriving from shrimp shells and characterized by abundant –OH and $–NH_2$ groups. Due to its high biocompatibility, biodegradability, hydrophilicity, good processability in films/hydrogels/sponges, mechanical strength and anti-bacterial properties, Ch and its composites have been widely exploited in drug and gene delivery, as well as in tissue engineering. Chitosan composites have been widely applied also in biosensing [1, 2], since Ch induces dispersion of the biological recognition element in a biomimetic environment, which improves both stability and lifetime of the sensor [3–5]. Examples of biosensors involving Ch also include enzymatic sensors for the analysis of glucose; since the detection in this case requires the presence of a redox active enzyme, namely glucose oxidase (Enz), they mainly consist of amperometric sensors. The enzyme, which is stably fixed on the electrode surface, converts glucose to the relevant oxidized form, according to (1):

$$\mathrm{D-Glucose} + \mathrm{O_2} \xrightarrow{\mathrm{Enz}} \mathrm{D-Gluconolactone} + \mathrm{H_2O_2}. \quad (1)$$

The amount of O_2 consumed by the enzymatic reaction and the amount of H_2O_2 consequently produced are proportional to the concentration of glucose in the sample and are detected by the electrode surface.

Amperometric detection of these species at conventional, flat electrode surfaces yields biosensors with rather poor performance, especially in terms of sensitivity and detection limit. For this reason, electrocatalytic

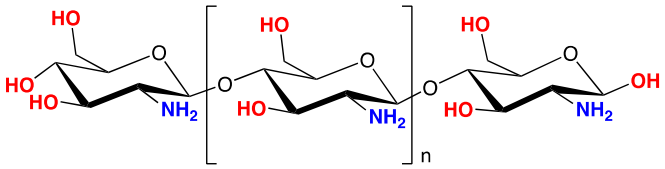

Scheme 1. Chemical structure of chitosan; –OH and –NH_2 functional groups are highlighted.

materials are often preferred, as they are capable to partially remove overvoltages implied in the charge transfer process and to shift the electrochemical process at less extreme potential values. Among the different materials tested to such a purpose, graphene oxide (GO) is now attracting the interest of the scientific community dealing with electrochemical sensing [6, 7]. This material, in fact, possesses a nanosized dimension, allowing a high number of oxidized residues to be well exposed to the surrounding environment. These moieties are responsible for the activation of effective electrocatalytic processes in charge of several species acting as the analyte [8–10]. These same can be also used as the binding sites of (bio)molecules, e.g. enzymes, antibodies, fragments of DNA, acting as the recognition element for a target analyte [11–13]. Except for these purposes specifically dealing with sensing, GO is often preferred to pristine graphene since it possesses greater solubility in many polar solvents, water included, and its surface chemistry can be easily tuned from highly oxidized, i.e. rich of epoxide, hydroxyl, carbonyl and carboxyl groups, to a structure possessing mainly sp^2-hybridized carbon atoms, thanks to a well-controlled electrochemical reduction [10, 14].

Recently, the appealing properties of both GO and Ch were synergistically used for the preparation of the relevant nanocomposites [15, 16]. The stability of these composites, formed by simply mixing the two components, was ascribed to adsorptions involving the positively charged $-NH_3^+$ groups of Ch on negatively charged GO nanosheets. The so-obtained stable dispersions were easily processed into the desired structures to be applied in different fields. Examples include the application as nanofibers [17] and as packaging films [18], exploiting the thermo-mechanical properties of the composite, or in drug delivery systems [19, 20] and for water purification [21] and remediation [22, 23], taking advantage of the recognized biocompatibility and low toxicity of the composites. As a consequence of the advantages previously highlighted, blends of Ch and GO were also successfully applied in electrochemical biosensing [24–29]. In particular, recent results demonstrated the potential application of a GO/Ch/Enz nanocomposite for glucose detection [24]. The sensing strategy adopted in this case was based on the electrocatalytic reduction of O_2, ascribable to the presence of GO in the electrode coating. Although similar effect was already acknowledged for carbon-based nanomaterials [30, 31] there is not a clear answer about which species plays an active role in this process [32–34]. The main advantage implied in the use of the GO/Ch/Enz nanocomposite proposed by Kang *et al* [24] was the possibility to detect glucose in the negative potential window, where the interference due to electroactive species normally present in real matrices, e.g. ascorbic acid, is quite limited.

Several examples reported the added value of using GO and Ch blends: Ch possesses a high number of amine residues that can be exploited for covalent grafting of GO [35–40] through amidation reaction with the carboxylic moieties or epoxide ring opening [41]. While amidation requires activation of carboxyls, the epoxide ring opening by primary amines can occur more easily, without activation, but it strongly depends on the amine structure, reaction time, pH and solvent [42]; for example, reaction of GO with polyethyleneimide occurred in water:EtOH 1:1 mixture under reflux for 24 h [43], reaction with TEG diamine occurred in DMF after five days [36], reaction with EDTA occurred in EtOH under sonication for 24 h at room temperature [44]. Thus, a simple mix of GO and Ch not necessary leads to a covalent composite.

Here, we aim at investigating a truly coherent composite, where GO and Ch are linked together by covalent bonds. This strategy could improve the loading and the stability of the enzyme on the sensor surface, and thus the performance of the device

Here, we propose a GO-based material consisting of GO covalently modified with Ch brushes, hereafter defined as GO−Ch. Amidation reaction was exploited to activate the carboxylic acids and to graft the abundant amine groups of Ch to GO [35]. In such conditions, concomitant epoxide ring opening could also occur, thus maximizing the degree of Ch modification. We demonstrate, by spectroscopic investigations, that chemical modification of GO induces significant increase of the number of amine moieties, which are useful to stably anchor a biological recognition element; at the same time, the chemical reaction induces partial reduction of GO, thus ultimately increasing the conductivity of the material with respect to a mere blend of Ch and GO (GO+Ch).

The GO–Ch nanocomposite was deposited on commercial screen-printed electrodes (SPE) and used as the substrate for immobilization of Enz by glutaraldehyde cross-linking. Sensing capability toward glucose

detection was also investigated, demonstrating the improvement of the analytical performance of the covalently modified GO with respect to a mixture of GO and Ch (GO+Ch) [24], and also to pristine GO after performing the electrochemical reduction to increase the conductivity [10].

2. Experimental

Medium molecular weight Ch (M_n = 190–310 kDa, 75%–85% deacetylated), lithium chloride (LiCl), anhydrous N,N-dimethylformamide (DMF), D-glucose, glutaraldehyde 25% solution, Nafion 5% solution and Enz (from *Aspergillus Niger*, type VII, lyophilized powder) were purchased from Sigma-Aldrich. Thionyl chloride ($SOCl_2$) was purchased from Acros, N,N-dimethylacetamide (DMAc) was purchased from Merck, and GO flakes were obtained by drying (Caution, the product may explode during this phase [45]) a commercial solution (4 mg ml^{-1}) purchased from Graphenea.

2.1. Synthesis of GO−Ch

GO (0.1 g) was dispersed in DMF (1.5 ml) by sonication for 1 h under N_2 atmosphere, then $SOCl_2$ (6 ml) was added and the resulting suspension was stirred at 80 °C for three days. The solvent was removed under vacuum and the crude acyl chloride-functionalized GO (GO−Cl) was recovered under N_2 atmosphere and used shortly after. Ch (0.5 g) was added to 20 ml of DMAc solution of LiCl (1.0 g) and the mixture was stirred at 130 °C for 2 h under N_2. GO−Cl was then added at room temperature (caution to exothermic reaction for $SOCl_2$ residual) and the reaction was carried out at 120 °C for two days. The resulting crude GO–Ch was poured into 100 ml of water and centrifuged. The solid obtained was washed with a solution of water and 5% acetic acid for several times, then rinsed with H_2O, acetone (RPE) and finally with Et_2O. The black powder was dried at 50 °C in oven overnight to obtain 0.19 g of GO−Ch.

1 mg ml^{-1} homogeneous dispersions of GO−Ch were obtained by one hour sonication in a ultrasonic bath (Bandelin Sonorex, 80 W); the suspension was placed in a bath with water and ice renewed every ten minutes to avoid excessive heating of the solution, which may modify functionalized GO foils in an irreproducible manner.

2.2. Preparation of the control sample for spectroscopic analysis (GO−Ch_ctrl)

Ch (0.25 g) was added to 10 ml of DMAc solution containing LiCl (0.5 g) and stirred at 130 °C for 2 h under N_2. After cooling down to room temperature, GO suspension (0.05 g in 1 ml of DMF sonicated for 1 h) was poured into the solution. The reaction was conducted at 120 °C for two days under N_2. The resulting crude mixture of GO−Ch_ctrl was poured into 30 ml of water and centrifuged; the solid obtained was washed with solution of water and 5% acetic for several times, then rinsed with water, acetone (RPE) and finally with Et_2O. The black powder was dried to oven 50 °C overnight obtaining 0.045 g of GO−Ch_ctrl.

2.3. Preparation of the reference samples for electrochemical analysis: GO and GO+Ch blend

Homogeneous dispersions of GO were obtained by diluting to 1.0 mg ml^{-1} the commercial GO suspension with deionized water and by sonicating the solution for 10 min

GO+Ch blend was obtained according to the procedure reported by Kang *et al* [24] by simply mixing GO and Ch. Briefly, a 1% (w/w) Ch solution was obtained by completely dissolving Ch in 0.2 M HCl solution by mild heating and the pH was then neutralized with NaOH. The blend suspension was obtained by suitable dilution of the commercial GO suspension with the Ch solution to finally obtain a 1 mg ml^{-1} GO solution also containing 0.5% of Ch. The mixture was mildly sonicated to obtain a homogeneous suspension.

2.4. X-ray photoelectron spectroscopy (XPS)

High-resolution XPS spectra were acquired by using a Phoibos 100 hemispherical energy analyzer (Specs GmbH, Berlin, Germany), equipped with Mg Ka radiation source ($\hbar\omega$ 1253.6 eV; power = 125 W). The analyzer was set in the constant analyzer energy mode, with pass energy of 40 eV. An overall resolution of 1.5 eV was measured and the analyzer was calibrated by the Ag 3d 5/2 (368.3 eV) and Au 4f 7/2 (84.0 eV) signals from freshly Ar^+ sputtered samples. Charging effects were corrected by calibration of Binding Energy on C 1s (284.8 eV) for all spectra. S 2p signal was fitted by doublets, with fixed spin–orbit shift (1.18 eV).

XPS samples were prepared by fixing the tablets prepared from the dry powders of each material on the sample, holed by conductive carbon tape. Base pressure in the analysis chamber during analysis was maintained at 1×10^{-9} mbar. Data analysis and fitting were performed with CasaXPS software, after Shirley background subtraction.

2.5. Scanning electron microscopy (SEM)

SEM analysis of all materials prepared was performed with SEM LEO 1530 FEG. The morphology of the electrode surfaces after the deposition of either GO−Ch or GO+Ch coatings was investigated by a Quanta-200 environmental scanning electron microscope (FEI Company), working in low vacuum conditions, equipped with an energy dispersive spectrometer (X-EDS, Oxford INCA-350).

2.6. X-ray diffraction (XRD)

XRD scans were carried out with PANanalytical X'Pert diffractometer in Bragg Brentano geometry. A copper target supplied a wavelength of 0.154 18 nm; data were collected for 50 s each 0.066° (2θ) with an X'Celerator detector.

2.7. Electrochemical setup

All the electrochemical measurements were performed with an Autolab PGSTAT12 potentiostat/galvanostat, from Metrohm-Ecochemie. SPEs were acquired from Metrohm-DropSens and consisted of a 4 mm diameter graphite working electrode, a graphite auxiliary electrode, and an Ag pseudo-reference electrode. The potential of the pseudo-reference electrode was fixed by adding 0.1 M KCl to all solutions used for the electrochemical tests.

All solutions for electrochemical tests were obtained in deionized water possessing a resistance of 18 MΩ cm. Electrochemical analyses were performed at room temperature and in solutions in equilibrium with the atmosphere, i.e. in the presence of O_2.

2.8. Preparation of Enz-based sensors

6.0 μl of the dispersions of GO−Ch, GO+Ch or GO were drop-cast on the working electrode of the SPE and the solvent was allowed to evaporate at room temperature.

Stable deposition of the enzyme on the electrode surface [46] was achieved by letting evaporate 5.0 μl of glutaraldehyde solution (1% in deionized water) on each GO-based coating for two hours, to allow cross-linking and covalent bonding to the nanomaterial. 6.7 μl of 10 mg ml^{-1} Enz solution, obtained in 0.1 M phosphate buffer (PBS) at pH 7.00, were drop-cast on the electrode surface and left drying at room temperature. Finally, 2.5 μl of a 1% pH-neutralized Nafion solution were drop-cast on the electrode surface. The electrodes were left drying overnight before the use.

Due to the poor conductivity of pristine GO, SPEs modified by such a nanomaterial were electrochemically treated at −1.25 V for 300 s in 0.1 M PBS [10] before the deposition of both glutaraldehyde and Enz, obtaining rGO coatings.

2.9. Electrochemical tests

Cyclic voltammetry (CV) responses in 0.5 mM ferrocenedimethanol (Fc), 0.1 M PBS (pH 7.00) were obtained to test the charge transfer resistance of different coatings. Deviation to the ideal 60 mV differences between the oxidation and relevant reduction peak, expected for this species undergoing a reversible oxidation process, indicates that the material possesses significantly higher charge transfer resistance with respect to conventional conductors of first species.

Preliminary electrochemical tests for glucose detection were carried out by CV, by performing four subsequent potential scans between −0.60 V and +0.40 V, at 0.02 V s^{-1} potential scan rate, in 0.1 M PBS (pH 7.00). Defined aliquots of a 20.0 mM glucose mother solution, obtained by dissolving glucose crystals in 0.1 M PBS, were then added to test the response of different modified electrodes with respect to the presence of such a species. The response at the steady state is reported for each CV measurement.

The performance of the different GO-based materials for glucose detection was defined by flow injection analysis (FIA). In this case, a constant potential of −0.40 V was applied by injecting glucose solutions at concentration levels ranging between 0.05 and 10 mM. Constant flow of 0.1 M PBS was kept at 1.0 ml min^{-1} using a Minipuls 3 (Gilson) peristaltic pump. First, 1.3 mM glucose solution was injected twenty times on the same device, in order to test repeatability of the sensor. Then, solutions at different concentration levels were analyzed randomly, in order to define the sensitivity of the sensor and to highlight the possible occurrence of memory effects; each solution was injected at least four times on the same SPE to test the sensor repeatability at different concentration levels. This procedure was repeated on three SPEs obtained in the same conditions to test the sensor reproducibility.

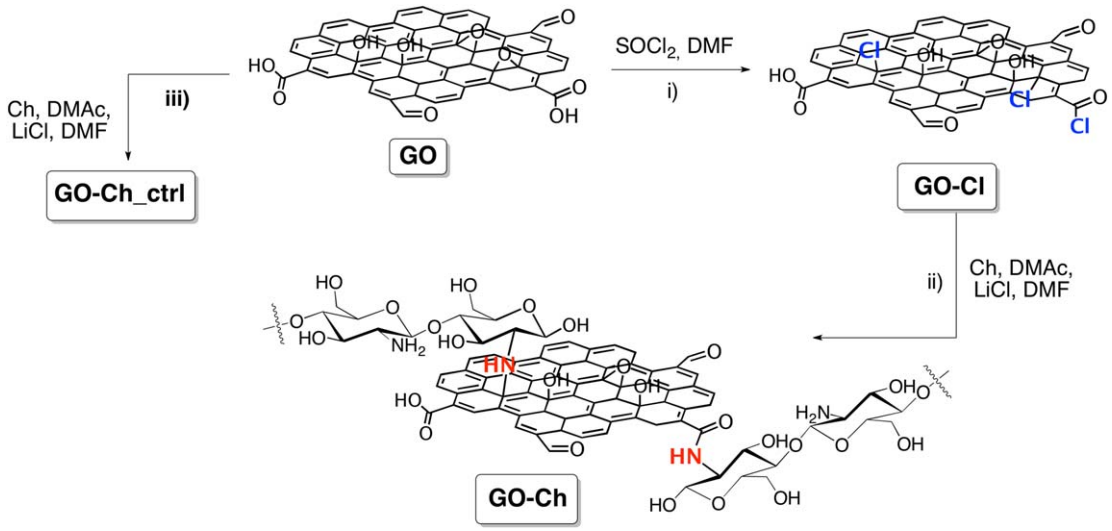

Scheme 2. Synthesis of GO−Ch: (i) activation of carboxylic groups; (ii) coupling with the amine groups of chitosan; (iii) mix of C and GO in DMF. A simple mixture called GO−Ch_ctrl, was also prepared as reference for the spectroscopic measurements. Chlorination of OH groups and epoxide ring opening concomitant reactions cannot be excluded and are also taken into account in the sketch.

3. Results and discussion

3.1. Synthesis and characterization

Covalent grafting of Ch on GO was achieved by esterification reaction of activated carboxylic groups of GO with the amine groups of chitosan, as previously described by Yang *et al* [47] and as summarized in scheme 2. However, as already discussed before, epoxide ring opening by the primary amines does likely occur.

FT-IR spectra of GO−Ch and of pristine GO and of Ch (figure S1 in ESI) show the disappearance of the carbonyl peaks (C=O) at 1729 cm^{-1} and spectrum changes in the secondary amide region (N–H bending) between 1550 and 1650 cm^{-1}, confirming the successful covalent grafting. Also, TGA analysis (figure S2 in ESI) is consistent with the formation of strong interactions between the two components, as shown by the enhanced thermal stability of GO−Ch, which decomposed slower with respect to Ch and GO.

XPS was performed on GO, GO–Cl, Ch and GO−Ch samples; the spectra are reported in figure 1 and figure S3 in ESI, whereas the abundance of the different functional groups, defined on the basis of the binding energy of the different functional groups (table S1, ESI), are reported in table S2 in ESI.

The C 1s spectrum of GO (figure S3a in ESI) is consistent with the typical structure of this material: the C–C sp^2 regions are surrounded by oxidized C–O functional groups, as confirmed by the deconvolution of the C 1s XPS signal [48].

Activated GO (GO–Cl) presents a 2.1% amount of chlorine (figure 1(g), Cl $2p_{3/2}$ B.E. 200.3 eV), compatible with the benzonyl chloride group [49], and in agreement with the relative amount of carbonyl group observed in C 1s (c.a. 3%) of pristine GO. $SOCl_2$ induces a secondary modification on GO, that can be ascribed to a partial reduction of GO: the O/C ratio, obtained from O 1s and C 1s area (O/C_{area}), goes from 0.36 ± 0.01 in GO to 0.07 ± 0.01 in GO–Cl. In order to confirm that C(O)–Cl functionalities can be attached to carboxylic group in GO, the $SOCl_2$ activation of Ch was also performed. The presence of Cl on the Ch–Cl adduct is significantly lower with respect to GO (0.3% Cl $2p_{3/2}$ B.E. 200.4 eV, spectrum not shown). On the other hand, a significant amount (6.8%) of the S 2p signal was also found for Ch–Cl sample, in the correspondence of the binding energy of S $2p_{3/2}$, and in particular at 164.2 eV that is in the correspondence of the signal expected for S–C covalent bonds [50]. The formation of this bond is probably ascribable to the high reactivity of $SOCl_2$ [51]. A small amount (0.4%) of S–C bond was also found for GO–Cl (figure 1(m)).

In GO−Ch, the presence of C(O)–NH–C bond between GO and Ch [35, 47, 52] was firstly confirmed by decrease of Cl 2p associated to R–C(O)–Cl from 2.1% in GO–Cl (figure 1(g)) to 0.3% in GO−Ch (figure 1(e)). In addition, the increase of N 1s peak from 0.3% in GO (figure 1(d)) up to 6% GO−Ch (figure 1(a)) and a significant chemical shift (399.5 eV in pristine Ch to 400.5 eV in GO−Ch) was observed in accordance with similar compounds previously reported: GO−Ch described in [47] or, more generally, for the class of materials presenting the R–C(O)–NH–R bond, e.g. polyamic acid (N 1s 400.5 eV) [53] and polyurethane (N 1s 400.3 eV) [54].

The actual formation of C–N covalent bond at GO−Ch was confirmed on the basis of XPS spectra acquired for the control sample, namely GO−Ch_ctrl (scheme 2). It presents approximately the same oxidation degree of

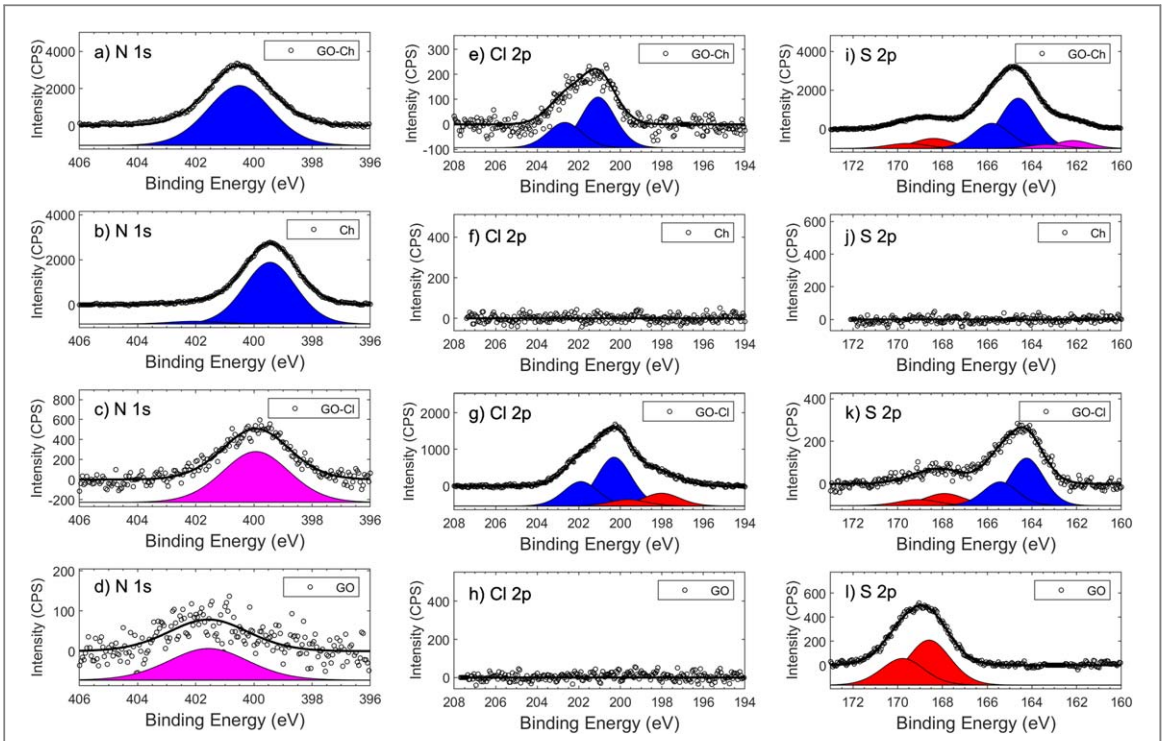

Figure 1. XPS signal of N 1s (a)–(d), Cl 2p (e)–(f) and S 2p (i)–(l) of GO–Ch (a), (e), (i), Ch (b), (f), (j), GO–Cl (c), (g), (k), GO (d), (h), (l). N 1s (a)–(d) presents C–N bond (blue) related to chitosan and other C–N groups due to DMF of residual on GO (magenta). Cl 2p (e)–(h) presents Cl–C(O)–R groups (blue) and other organic Cl groups (red). S 2p (i)–(l) presents S–O groups (red), S–C/S–N (blue) and unknown S–X group (magenta).

GO, supporting that the partial reduction of GO in GO−Ch is due to the effect of $SOCl_2$ treatment. The less intense N 1s peak (2.3% versus 6.0% in GO−Ch) is ascribed to the washing steps removing unreacted Ch and it confirms the covalent grafting of Ch on GO after the reaction.

SEM and XRD analyses investigated morphology and structure of GO−Ch, respectively. SEM images (figure S4, ESI) show the typical morphology of GO flakes, which are not affected by the reaction. This suggests that all properties observed for the functionalized materials are ascribable to the surface chemical moieties.

XRD patterns of GO, GO−Ch and GO−Ch_ctrl are shown and compared in figure S5, ESI. A peak characterizes the GO pattern at 9.98° (2θ). It is indexed as (001) of GO or (002) as derived from graphite structure. In any case, it represents the interlayer spacing between carbon layers: 0.89 nm in this sample. Its complete disappearance in GO−Ch_ctrl sample can be ascribed to of the reduction of all oxygen functionalities; furthermore the broad band centered around 20° confirms the absence of ordered aggregation and the full dispersion of graphene-like sheets on Ch support. On the contrary, in GO−Ch sample the lack of the peak typical of GO and the presence of a broad peak at 25.2° state the disruption of GO layered structure, but with a partial aggregation of the sheets at distances nearby 0.35 nm, i.e. close to the graphitic (002) interlayer distance of 0.34 nm.

3.2. Electrochemical measurements

To demonstrate the advantages offered by the use of a covalently-bonded Ch on GO material, we performed electrochemical tests on three different electrode coatings: (i) unfunctionalized rGO, i.e. a GO coating electrochemically reduced at −1.25 V [10], (ii) covalently-bonded GO−Ch, and (iii) GO+Ch blend. This last material was obtained by adopting a strategy already described in [24] and was used as a benchmark to highlight the advantages deriving from the chemical activation of oxygen-based moieties present on GO nanosheets to stably bind Ch molecules. Although the analytical performance of the GO+Ch blend was already discussed in the literature, electrochemical tests were repeated in the conditions defined by us, i.e. in FIA; this technique, in fact, was preferred since it reproduces the conditions adopted for the continuous monitoring of glucose, e.g. in on-line monitoring of body liquids, which can be useful for wearable sensors. In addition, the use of the same GO batch for the formulation of both GO−Ch and of GO+Ch blend allows a most proper comparison between these two materials.

Charge transfer resistance at the GO−Ch coating, in comparison to rGO and GO+Ch blend, was preliminarily tested in Fc solution before the deposition of Enz (figure 2). CV response obtained at GO−Ch shows a peak-to-peak separation of *ca*. 70 mV, meaning that this coating is suitable for electrochemical

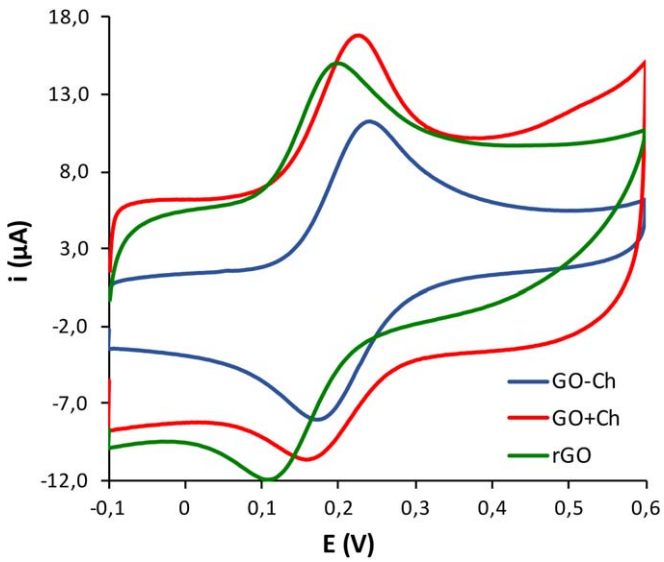

Figure 2. CV responses obtained by different modified electrodes in 0.5 mM Fc, 0.1 M PBS; 0.05 Vs^{-1} potential scan rate.

applications without the need for any electrochemical pre-treatment. A similar peak-to-peak separation was also obtained for the GO+Ch blend; this result let us conclude that the simple mixing of GO with Ch molecules induces ring opening of the epoxy groups on GO, sufficiently improving the conductivity of this material for the electrochemical purposes. Suitable conductivity of simple GO coatings was only obtained after electrochemical pre-treatment at −1.25 V [10]; this notwithstanding, the charge transfer resistance of the resulting rGO coating was slightly worse, as evident from a peak-to-peak separation of about 80 mV. CV responses of Fc oxidation recorded at GO−Ch at different scan rates show a linear relationship ($R^2 = 0.998$) between the anodic peak current and the square root of the potential scan rate (figure S6 in ESI), meaning that the charge transfer process is controlled by diffusion, as expected for a working electrode possessing performance suitable for the electroanalytical applications.

Electrochemical measurements performed at GO−Ch modified SPEs show the electrocatalytic effect induced by the presence of the coating toward oxygen reduction (see figure S7 in ESI): the voltammogram registered in atmospheric conditions, i.e. in the presence of oxygen, exhibits a reduction peak at −0.4 V significantly shifted at less negative potentials with respect to that obtained at the pristine, carbon-based, electrode surface. Quite interestingly, the sensitivity of O_2 reduction is higher when Ch is present inside the GO coating. This peak decreases when glucose is added to the solution (figure 3) as a consequence of the enzymatic reaction, according to (1). As a confirmation of this conclusion, GO−Ch modified electrodes not functionalized with Enz do not show any decrease of the oxygen reduction peak when tested in the presence of glucose (figure S8 in ESI).

The voltammograms in figure 3 also highlight the possible quantification of glucose by this sensor system, as the peak decreasing is proportional to the amount of glucose in solution; these results are in agreement with those previously reported for GO+Ch modified electrodes [24].

Calibration plots for glucose detection were obtained by FIA (figure 4); for this reason, an outermost film of Nafion was added in order to hinder the mechanical detachment of the whole GO-based coating from the underlying working electrode surface. Similar modified SPEs, in fact, were also tested without Nafion film, but in this case only a rather poor correlation was obtained between the current registered and the concentration of glucose.

The repeatability of the sensor response was checked by twenty subsequent injections of the 1.3 mM glucose solution, representing the centroid of the calibration curve (see hereafter). The mean relative standard deviation (RSD%) calculated from the responses of three SPEs modified by either GO−Ch or GO+Ch was 6.2% and 5.3%, respectively. These relatively low values confirm the good stability of the overall coating, even considering the Enz on the GO film, in the conditions chosen.

The analytical performance of the three materials was calculated on the basis of calibration plots similar to those reported in figure 4(b). The response of the sensor was obtained by four subsequent injections at each concentration level, also to test the repeatability of the sensor in the whole calibration plot; in all cases the evaluated RSD% resulted well below 5%, showing a very high repeatability degree of all the coatings tested. The results finally reported in table 1 are obtained by considering the responses of three SPEs, deposited and tested in

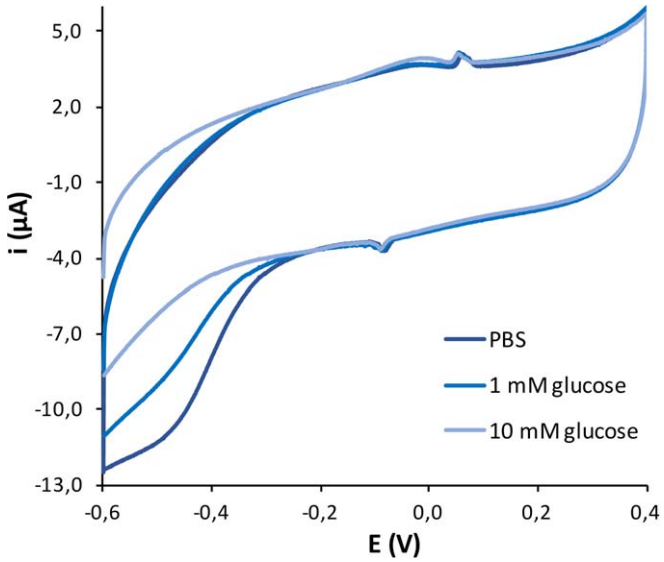

Figure 3. Typical CV responses obtained at GO−Ch and Enz modified SPE in 0.1 M PBS in absence and in presence of glucose.

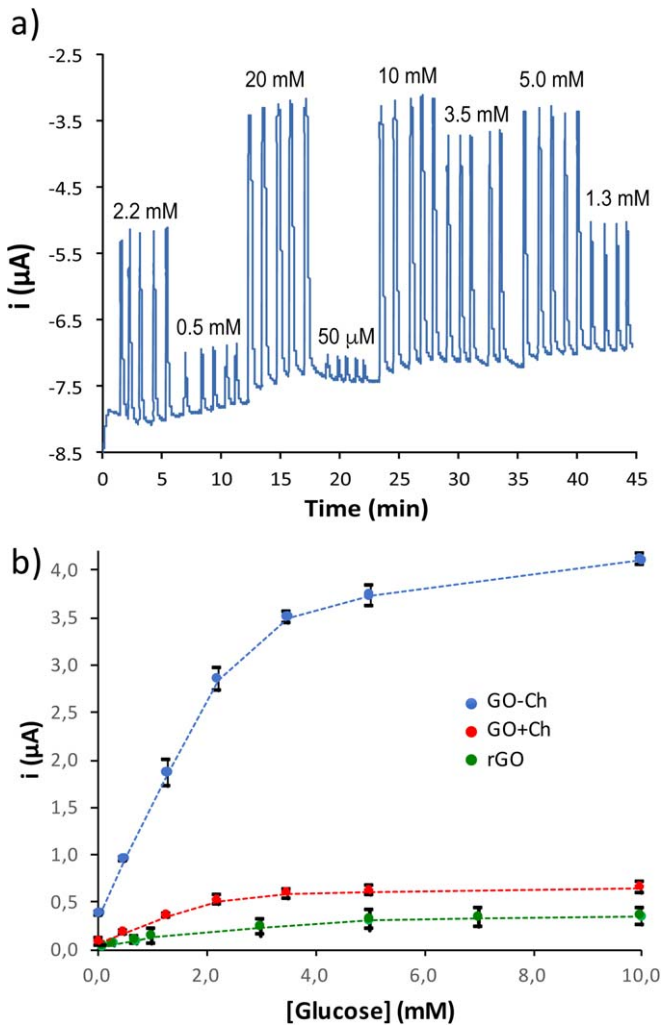

Figure 4. (a) Typical amperometric response recorded at GO−Ch modified SPE in FIA by polarizing the electrode at the fixed potential of −0.4 V; concentration of the solutions of glucose injected during time is reported in the correspondence of the relevant signals obtained. (b) Relevant calibration plot obtained at GO–Ch modified SPE in relation to responses obtained at GO+Ch and modified electrodes.

Table 1. Analytical performance on the different coatings tested. Results for each coating are obtained from three electrodes tested in the same conditions.

	GO−Ch	GO+Ch	rGO
Sensitivity (μA mM^{-1} cm^{-2})	7.61	1.64	0.94
Linearity range (mM)	0.5–3.5	0.5–2.2	0.5–2.2
RSD_{slope} (%)	9.8	15.5	63.1

the same conditions for each of the three materials tested. As observed, GO−Ch shows significantly higher sensitivity when compared to both pristine rGO and to non-covalently bonded GO+Ch blend, as defined by a Student's t-test ($p = 0.95$). The higher sensitivity can be also ascribed by the higher homogeneity of GO−Ch coating with respect to GO+Ch (see section S8 in ESI).

Reproducibility of the sensor building up was defined by considering the RSD of the sensitivity (i.e. the slope) of calibration plots obtained from three SPEs obtained and tested in the same conditions. As observed from the resulting RSD_{slope} values (table 1), the responses obtained at GO−Ch electrodes are quite reproducible.

4. Conclusions

Our work shows that covalent modification of GO with Ch provides a material suitable for glucose sensing that outperforms the not covalently modified analogues. The synthetic protocol adopted is a standard method, allowing covalent modification of GO through an amidation reaction. The advantages of this approach rely on the increase of the number of active sites to bind the glucose oxidase enzyme and on the partial reduction of GO, which occurs during the carboxyl groups activation; this was demonstrated by synthesizing a tailored control sample (GO−Ch_ctrl). The biosensor obtained by drop-casting GO−Ch shows enhanced sensitivity and higher reproducibility with respect to the sensor developed by using a mere mixture of GO and Ch (GO+Ch) previously reported in literature. Despite a proper definition of the performance of the GO−Ch based sensors can be only carried out after testing the sensor in real conditions, the linearity range found (see table 1) suggests the possible use of the device as a wearable sensors for the continuous monitoring of glucose in sweat. In this respect, the flow analyses described in this paper evidence that this application is well feasible for at least one hour of measurements without significant variation of the sensor repeatability.

Acknowledgments

The research leading to these results has received funding from the European Union's Horizon 2020 research and innovation programme under GrapheneCore2 785219—Graphene Flagship and from the Swedish Research Council under project (project Janus 2017-04456).

ORCID iDs

Fabrizio Poletti https://orcid.org/0000-0001-9646-021X
Alessandro Kovtun https://orcid.org/0000-0002-7614-7100
Vincenzo Palermo https://orcid.org/0000-0002-0168-9693
Chiara Zanardi https://orcid.org/0000-0002-2091-3398
Manuela Melucci https://orcid.org/0000-0003-2326-0094

References

[1] Baranwal A, Kumar A, Priyadharshini A, Oggu G S, Bhatnagar I, Srivastava A and Chandra P 2018 *Int. J. Biol. Macromolecules* **110** 110
[2] Kubáň P, Foret F and Erny G 2019 *Electrophoresis* **40** 2084
[3] Suginta W, Khunkaewla P and Schulte A 2013 *Chem. Rev.* **113** 5458
[4] Kang X, Mai Z, Zou X, Cai P and Mo J 2007 *J. Nanosci Nanotechnol.* **7** 1618
[5] Kaur N, Bharti A, Batra S, Rana S, Rana S, Bhalla A and Prabhakar N 2019 *Microchemical J.* **144** 102
[6] Lawal A T 2015 *Talanta* **131** 424
[7] Shao Y, Wang J, Wu H, Liu J, Aksay I A and Lin Y 2010 *Electroanalysis* **22** 1027
[8] Bonanni A, Ambrosi A, Chua C K and Pumera M 2014 *ACS Nano* **8** 4197
[9] Hui K W, Pumera M and Bonanni A 2015 *Chem. Eur. J.* **21** 11793
[10] Maccaferri G, Zanardi C, Xia Z Y, Kovtun A, Liscio A, Terzi F, Palermo V and Seeber R 2017 *Carbon* **120** 165
[11] Tudose M *et al* 2019 *Appl. Surf. Sci.* **471** 553

[12] Kansara V, Patil R, Tripathi R, Jha P K, Bahadur P and Tiwari S 2019 *Colloids Surf.* B **173** 421
[13] Makharza S, Cirillo G, Bachmatiuk A, Ibrahim I, Ioannides N, Trzebicka B, Hampel S and Rümmeli M H 2013 *J. Nanopart Res.* **15** 2099
[14] Ambrosi A and Pumera M 2013 *Chem. Eur. J.* **19** 4748
[15] Fang M, Long J, Zhao W, Wang L and Chen G 2010 *Langmuir* **26** 16771
[16] Yang X, Tu Y, Li L, Shang S and Tao X-M 2010 *ACS Appl. Mater. Interfaces* **2** 1707
[17] Cao L, Zhang F, Wang Q and Wu X 2017 *Mater. Sci. Eng.* C **79** 697
[18] Ahmed J, Mulla M, Arfat Y A and Thai T L A 2017 *Food Hydrocolloids* **71** 141
[19] Abbasian M, Roudi M-M, Mahmoodzadeh F, Eskandani M and Jaymand M 2018 *Int. J. Biol. Macromolecules* **118** 1871
[20] Zhang H, Yan T, Xu S, Feng S, Huang D, Fujita M and Gao X-D 2017 *Mater. Sci. Eng.* C **73** 144
[21] Chen Y, Chen L, Bai H and Li L 2013 *J. Mater. Chem.* A **1** 1992
[22] Kamal M A, Bibi S, Bokhari S W, Siddique A H and Yasin T 2017 *Reactive Funct. Polym.* **110** 21
[23] Ali M E A 2018 *Arab. J. Chem.* **11** 1107
[24] Kang X, Wang J, Wu H, Aksay I A, Liu J and Lin Y 2009 *Biosens. Bioelectron.* **25** 901
[25] Tiwari I, Singh M, Pandey C M and Sumana G 2015 *Sensors Actuators* B **206** 276
[26] Singh J *et al* 2013 *Process Biochemistry* **48** 1724
[27] Cai C-J, Xu M-W, Bao S-J, Lei C and Ji D-Z 2012 *RSC Adv.* **2** 8172
[28] Zhou K, Zhu Y, Yang X, Luo J, Li C and Luan S 2010 *Electrochim. Acta* **55** 3055
[29] Wu K-H, Wang D-W and Gentle I R 2014 *Carbon* **73** 234
[30] Wang D-W and Su D 2014 *Energy Environ. Sci.* **7** 576
[31] Rivera L M, García G and Pastor E 2018 *Curr. Opin. Electrochem.* **9** 233
[32] Sarapuu A, Kibena-Põldsepp E, Borghei M and Tammeveski K 2018 *Mater. Chem.* A **6** 776
[33] Ahmed M S and Kim Y-B 2017 *Carbon* **111** 577
[34] Wang L, Chua C K, Khezri B, Webster R D and Pumera M 2016 *Electrochem. Commun.* **62** 17
[35] Bao H, Pan Y, Ping Y, Sahoo N G, Wu T, Li L, Li J and Gan L H 2011 *Small* **7** 1569
[36] Bustos-Ramírez K, Martínez-Hernández A L, Martínez-Barrera G, De Icaza M, Castaño V M and Velasco-Santos C 2013 *Materials* **6** 911
[37] Ryu H J, Mahapatra S S, Yadav S K and Cho J W 2013 *Eur. Polym. J.* **49** 2627
[38] Hu H, Wang X, Wang J, Liu F, Zhang M and Xu C 2011 *Appl. Surf. Sci.* **257** 2637
[39] Sun H, Zhang L, Xia W, Chen L, Xu Z and Zhang W 2016 *Appl. Phys.* A **122** 632
[40] Emadi F, Amini A, Gholami A and Ghasemi Y 2017 *Sci. Rep.* **7** 42258
[41] Vacchi I A, Spinato C, Raya J, Bianco A and Ménard-Moyon C 2016 *Nanoscale* **8** 13714
[42] Kasprzak A, Zuchowska A and Poplawska M 2018 *Beilstein J. Org. Chem.* **14** 2018
[43] Pakulski D, Czepa W, Witomska S, Aliprandi A, Pawlu´c P, Patroniak V, Ciesielski A and Samori P 2018 *J. Mater. Chem.* A **6** 9384
[44] Yang A, Li J, Zhang C, Zhang W and Ma N 2015 *Appl. Surf. Sci.* **346** 443
[45] Qu Y, Guo F and Hurt R 2014 *Carbon* **72** 215
[46] Guisan J M 2013 *Immobilization of Enzymes and Cells* (Totowa, NJ: Humana Press) pp 33–41
[47] Yang Q, Pan X, Clarke K and Li K 2012 *Ind. Eng. Chem. Res.* **51** 310
[48] Kovtun A, Jones D, Dell'Elce S, Treossi E, Liscio A and Palermo V 2019 *Carbon* **143** 268
[49] Gassman P, Macomber D W and Willging S M 1985 *J. Am. Chem. Soc.* **107** 2380
[50] Lindberg B J, Hamrin K, Johansson G, Gelius U, Fahlman A, Nordling C and Siegbahn K 1970 *Phys. Scr.* **1** 286
[51] El-sakka I A and Hassan N A 2005 *J. Sulfur Chem.* **26** 33
[52] Dreyer D R, Todd A D and Bielawski C W 2014 *Chem. Soc. Rev* **43** 5288
[53] Russat J 1988 *Surf. Interface Anal.* **11** 414
[54] Beamson G and Briggs D 1992 *High Resolution XPS of Organic Polymers—The Scienta ESCA300 Database* (New York: Wiley)